Vol. 34 (2003) *ACTA PHYSICA POLONICA B* No 2

FILLED SKUTTERUDITES: FORMATION, GROUND STATE PROPERTIES AND THERMOELECTRIC FEATURES*

E. Bauer, St. Berger, M. Della Mea, G. Hilscher, H. Michor
Ch. Paul

Institute of Solid State Physics, Vienna University of Technology
1040 Wien, Austria

A. Grytsiv, P. Rogl

Institute of Physical Chemistry, University Vienna, 1090 Wien, Austria

E.W. Scheidt

Lehrstuhl für Experimentalphysik III, University Augsburg
86159 Augsburg, Germany

C. Godart

CNRS-UPR209, ISCSA, 94320 Thiais, France

and M. Abd Elmeguid

II. Physikalisches Institut, University Cologne, 50937 Köln, Germany

(Received July 10, 2002)

Filled skutterudites $RETM_4X_{12}$ with RE = rare earth, TM = transition metal and X = pnictogen represent a class of complex materials exhibiting a broad variety of ground state properties. These model systems also allow to tailor the charge carrier density in order to optimise the thermoelectric performance with respect to its applicability in both, energy conversion and cooling processes. The present review focuses mainly on strong electron correlations in such compounds and their effect on thermoelectric properties.

PACS numbers: 75.30.Mb, 74.25.Bt, 75.30.Cr

---

[*] Presented at the International Conference on Strongly Correlated Electron Systems, (SCES 02), Cracow, Poland, July 10–13, 2002.

1. Introduction

In the past few years, renewed interest was directed to new classes of complex materials feasible with respect to thermoelectric applications. Among such multinary systems are skutterudites $\mathrm{RE_yTM_4X_{12}}$ with RE = rare earth, TM = transition metal and X = pnictogen, crystallising in the $\mathrm{LaFe_4P_{12}}$ structure, a filled ternary derivative of cubic $\mathrm{CoAs_3}$ [1].

Depending on the particular rare earth element, features like superconductivity, long range magnetic order, heavy fermion, non-Fermi-liquid, intermediate and mixed valence behaviour or hopping conductivity were found [2].

Significant interest in this family of compounds, however, stems from the fact that filled skutterudites are potential candidates for thermoelectric applications. Materials considered for such a purpose should exhibit large values of the *figure of merit* ZT ($ZT = S^2T/(\rho\lambda)$, T ...temperature, S ...Seebeck coefficient, ρ ...electrical resistivity and λ ...thermal conductivity). Depending on the carrier concentration and on particular interaction mechanisms present in a particular sample, Seebeck values well above 100 μV/K are observed. Besides, ternary skutterudites are outstanding with respect to their low thermal conductivity which, in some cases, can be near the theoretical lower limit. As a matter of fact, the dramatically diminished $\lambda(T)$ values refer to an exceptionally large thermal parameter of the loosely bound rare earth element, corresponding to a "rattling" (*i.e.*, soft phonon mode) of this atom in an oversized cage [3].

In the present paper we will review a number of physical properties related to electron correlations and we will show how transport and thus the thermoelectric performance is modified by interaction processes like Kondo scattering, intermediate valence or crystal field splitting. The latter phenomena are frequently found in filled skutterudites based on Ce, Pr, Eu and Yb.

2. Formation of skutterudites

Filled skutterudites crystallise in the cubic $\mathrm{LaFe_4P_{12}}$ type structure, which is a filled ternary derivative of cubic $\mathrm{CoAs_3}$ [4]. The transition elements (TM) occupy the 8c position and the pnictogen atoms (X) are found on the 24h. Together octahedras are formed that are slightly tilted with respect to each other. The octahedra create large voids in the structure, that are able to accommodate electropositive elements (EP) such as rare earths or alkali metals. These filler elements, however, are just loosely bound in the cages, giving rise to low energy optical modes [5]. A systematic investigation concerning the formation of skutterudites is summarised in Fig. 1, revealing 7 different groups of unfilled skutterudites. The first group contains samples

Formation of Skutterudites EPT_4X_{12}

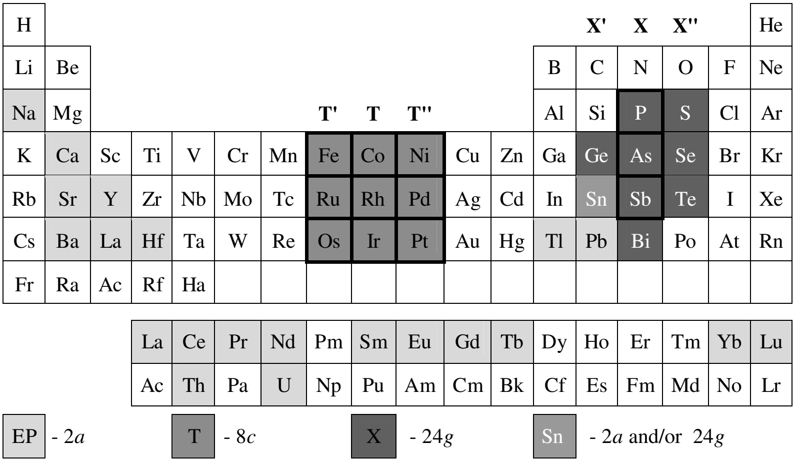

unfilled skutterudites

binary			*ternary*			
T_4X_{12}	**T'_4X_{12}**	**T''_4X_{12}**	**$T_2X'_6X''_6$**	**$T'_2T''_2X_{12}$**	**$T'_4X_8X''_4$**	**$T''_4X_8X'_4$**
Co_4P_{12} Co_4As_{12} Co_4Sb_{12} Rh_4P_{12} Rh_4As_{12} Rh_4Sb_{12} Ir_4P_{12} Ir_4As_{12} Ir_4Sb_{12}	"Fe_4Sb_{12}"	Ni_4P_{12} Pd_4P_{12}	$Co_4Ge_6Te_6$ $Co_4Sn_6Se_6$ $Co_4Sn_6Te_6$ $Co_4Ge_6S_6$ $Co_4Ge_6Se_6$ $Rh_4Ge_6S_6$ $Ir_4Ge_6S_6$ $Ir_4Ge_6Se_6$ $Ir_4Sn_6S_6$ $Ir_4Sn_6Se_6$ $Ir_4Sn_6Te_6$	$Fe_2Ni_2Sb_{12}$ $Fe_2Ni_2As_{12}$ $Fe_2Pd_2Sb_{12}$ $Fe_2Pt_2Sb_{12}$ $Ru_2Ni_2Sb_{12}$ $Ru_2Pd_2Sb_{12}$ $Ru_2Pt_2Sb_{12}$	$Fe_4Sb_8Se_4$ $Fe_4Sb_8Te_4$ $Ru_4Sb_8Se_4$ $Ru_4Sb_8Te_4$ $Os_4Sb_8Te_4$	$Ni_4P_8Ge_4$ $Ni_4Bi_8Ge_4$ $Pt_4Sb_{7.2}Sn_{4.8}$ $Ni_4Sb_8Sn_4$ $Ni_4As_8Ge_4$

filled skutterudites

ternary	*Quaternary*	
EPT_4X_{12}	**$EPT'_4(X_{1-x}X'_x)_{12}$**	**$EP(T_{1-x}T'_x)_4X_{12}$**
T = Fe, Ru, Os **X = P, As, Sb** **EP**=Ca, Sr, Ba, La, Ce, Pr, Nd Sm, Eu, Gd, Tb, Yb, Th, U	**T' = Co, Ir** **X = Sb; X' =Ge, Sn** **EP** = La, Nd, Sm, Tl	**T = Fe; T' = Co** **X = Sb** **EP** = Tl
$LaFe_4P_{12}$, UFe_4P_{12}, $ThOs_4As_{12}$, $YbFe_4Sb_{12}$, ...	$LaIr_4Sb_9Ge_3$,$NdIr_4Sb_9Ge_3$, $SmIr_4Sb_9Ge_3$,$TlCo_4Sb_{11}Sn$, $La_{0.9}Co_4Sb_{10.3}Sn_{2.44}$, ….	$TlFeCo_3Sb_{12}$

metastable partially filled skutterudites:

$EP_{1-y}Fe_4Sb_{12}$; EP = Na, Y, Hf, Sn, Lu **$EP_{1-y}Co_4Sb_{12}$; EP = Sn, Pb**

Fig. 1. Formation of binary and ternary skutterudites.

formed by Co, Rh and Ir with P, As and Sb allowing all possible combinations. There is a total of 72 compensated electrons, thus the compounds are diamagnetic semiconductors. Both following groups are obtained by an exchange of TM with Fe, Ni, Pd. Metastable $FeSb_3$ exhibits 4 uncompensated holes as charge carriers while NiP_3 and PdP_3 possess 4 extra electrons, behaving therefore metallic. The fourth group contains compounds where pnictogen elements are emulated by "synthetic pnictogens", *i.e.*, an appropriate mixture of IVa and VIa elements. Distortions, however, may occur. A similar approach is possible with respect to 3d substitutions. In group six and seven, partial substitution on the pnictogen and on the TM site is observed.

The filled skutterudites can be divided into two different groups: *(i)* Compounds are formed by a simple filling of the 2a site of the framework built by 8c and 24h atoms. *(ii)* Electronically promoted formation of filled skutterudites. If the polyanion framework has less than 72 electrons, electrons provided by electropositive filler elements can stabilise the structure.

3. Transport, thermodynamic and magnetic properties

Physical properties of filled skutterudites depend in a subtle manner on the electropositive rare earth ion as filler element of the voids and on the carrier concentration as well as on the magnetic state of the transition metal–pnictogen sublattice. Moreover, the particular filling of a certain compound is of importance. In the following section we will outline a number of outstanding features of filled skutterudites where electron correlations may play a crucial role.

3.1. Heavy electron behaviour in Pr-based skutterudites

Besides the traditional materials explored with respect to strong electron correlations and heavy fermion behaviour due to Kondo interaction, such as, *e.g.*, $\mathrm{CeFe_4Sb_{12}}$ and $\mathrm{YbFe_4Sb_{12}}$, skutterudites based on Pr have recently been shown to exhibit a number of extraordinary low temperature anomalies. Just to mention a few, superconductivity was found in $\mathrm{PrRu_4As_{12}}$ and $\mathrm{PrRu_4Sb_{12}}$ below 2.4 and 1 K, respectively [6,7], a metal to insulator transition is obvious in $\mathrm{PrRu_4P_{12}}$ at $T_{\mathrm{MI}} = 60$ K [8]. Very recently, heavy fermion superconductivity was discovered in $\mathrm{PrOs_4Sb_{12}}$ with a transition temperature of 1.8 K. Specific heat studies suggest that the superconducting ground state is formed by heavy quasiparticles as concluded from a normal state Sommerfeld value γ of about 500 mJ/molK^2 [9].

$\mathrm{PrFe_4P_{12}}$ shows a phase transition at $T = 6.2$ K, which according to recent studies [2,10] is associated with a principal order parameter of, most likely, quadrupolar origin. Thus, Kondo-like anomalies found in transport phenomena as well as the huge $C_p/T(T \to 0)$ value of 1.4 J/molK^2 [11,12] may refer to a quadrupolar Kondo effect. Additionally, de Haas van Alphen measurements evidenced heavy electrons and unusual features of the Fermi surface topology [13], suggesting strongly correlated electrons in this compound.

Although Pr moments in skutterudites are almost localised, a significant hybridisation can originate from strong p–f mixing in conjunction with a large coordination number. Another possible source for a number of extraordinary features in such Pr-based skutterudites is that crystalline electric fields (CEF) cause a splitting of the $J = 4$ total angular momentum of non-Kramers ion Pr into a Γ_1 singlet, a Γ_3 doublet and in the Γ_4 and Γ_5 triplets. Both the Γ_1 singlet and the Γ_3 doublet are non-magnetic, *i.e.*, the projection of the magnetic moment J_z onto the Γ_3 state is zero; however, the electric quadrupolar moment $3J_z^2 - J(J+1)$ does not vanish. The conduction electrons can then, in principle, interact with the internal degrees of freedom associated with the quadrupolar moment of the Pr ion and this interaction can lift the ground state degeneracy. Ternary skutterudite $\mathrm{Pr_{0.73}Fe_4Sb_{12}}$, however, exhibits the magnetic triplet Γ_5 as CEF ground state, linked to a moment $\mu = 2\ \mu_\mathrm{B}$. Thus, long range magnetic order occurs at $T_\mathrm{mag} \approx 5.5$ K [14].

The heat capacity of $\mathrm{Pr_{0.73}Fe_4Sb_{12}}$, shown in Fig. 2 exhibits a pronounced anomaly around $T \approx 5$ K, indicating the onset of long range magnetic order. Increasing fields suppress the anomaly in $C_p(T)$, eventually vanishing for external fields higher than 3 T. At each field value, however, the low temperature heat capacity is remarkably high, resembling well known heavy fermion systems based on Ce, Yb or U as well as observations made for $\mathrm{PrFe_4P_{12}}$ [2].

At very low temperatures C_p/T of $\mathrm{Pr_{0.73}Fe_4Sb_{12}}$ displays a significant rise due to the nuclear heat capacity (inset, Fig. 2). This contribution is primarily attributed to the $I = 5/2$ state of Pr, referring to a strong intra-site hyperfine coupling between the nuclei and $4f$ electrons. At temperatures slightly above (≈ 1 K), C_p/T increases with external magnetic fields. Fluctuations of the order parameter prior to a phase transition or destroying of the ordered state by the magnetic field may cause such an enhancement. A similar trend of $C_p/T(H)$ was derived previously for $\mathrm{PrFe_4P_{12}}$ [2].

To estimate the characteristic temperature scale of the heavy quasiparticles associated with the large C_p/T values of $\mathrm{Pr_{0.73}Fe_4Sb_{12}}$, the resonance level model of Schotte and Schotte [15] is adopted. This model assumes a narrow Lorentzian density of states at the Fermi energy E_F with a width $\Delta \sim T_\mathrm{K}$, where the Kondo temperature T_K is supposed to represent the appropriate temperature scale which describes thermal excitations in a strongly renormalised quasiparticle band formed around E_F. A least squares fit to the experimental data is shown in Fig. 2(b) as solid line, yielding $T_\mathrm{K} \approx 25$ K. Furthermore, this model shows that the jump in the specific heat δ_c at the transition temperature is much smaller than expected *e.g.*, in a mean-field like description. Such a reduction, however, is well known in magnetically ordered Kondo lattices where δ_c is continuously diminished as T_K increases

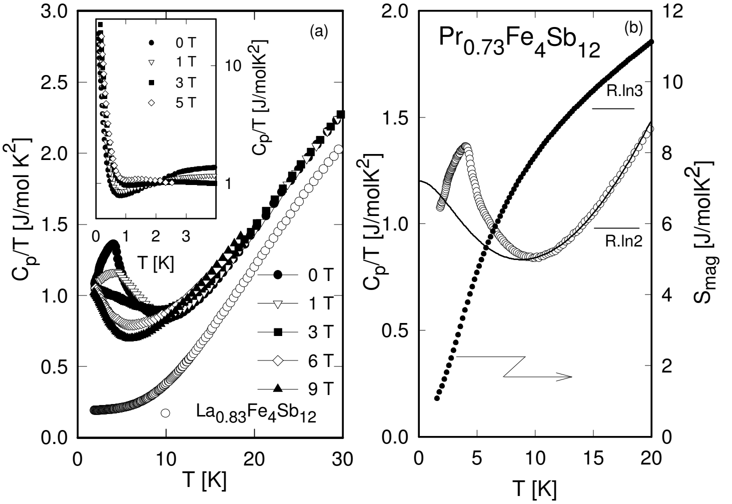

Fig. 2. (a) Temperature and field dependent heat capacity C_p/T *vs* T of $\mathrm{Pr}_{0.73}\mathrm{Fe}_4\mathrm{Sb}_{12}$. The inset shows low temperature features. (b) left axis: C_p/T *vs* T of $\mathrm{Pr}_{0.73}\mathrm{Fe}_4\mathrm{Sb}_{12}$ (opens circles) together with a least squares fit (solid line) according to the model of Schotte and Schotte; right axis: magnetic entropy S of $\mathrm{Pr}_{0.73}\mathrm{Fe}_4\mathrm{Sb}_{12}$.

with respect to the magnetic interaction strength. Some broadening of the phase transition anomaly may arise from inhomogeneities and/or the partly filled cages of the structure.

The magnetic entropy S_{mag} of $\mathrm{Pr}_{0.73}\mathrm{Fe}_4\mathrm{Sb}_{12}$ is derived by a comparison with $\mathrm{La}_{0.83}\mathrm{Fe}_4\mathrm{Sb}_2$. Results of $S_{\mathrm{mag}}(T)$ are shown in Fig. 2(b), right scale. The ground state degeneracy of the Pr ion is lifted either by magnetic ordering and/or by Kondo interaction, responsible for the large effective electron masses. The entropy release is found to be $R\ln 2$ at about 7 K and $R\ln 3$ around 13 K, in line with the Γ_5 triplet as ground state and the nonmagnetic singlet Γ_1 situated about 30 K above.

3.2. Intermediate and mixed valence behaviour in Eu-based skutterudites

Intermediate and mixed valence of the filler elements can provide a possibility to tune in a subtle manner the carrier concentration of a certain skutterudite and thus can determine electronic transport to a large extent. Moreover, valence fluctuations are considered to be an effective mechanism to reduce the lattice thermal conductivity as phonons are strongly scattered on differences of valence states [1]. Moreover, intermediate and mixed valence, in particular of the filler elements, also modify magnetic properties of the system.

A novel phenomenon is the occurrence of mixed valence in $\mathrm{Eu(Fe,Co)_4Sb_{12}}$ although skutterudites possess just one lattice site for Eu. Shown in Fig. 3 are L_{III} spectra and Mössbauer measurements performed on $\mathrm{Eu_{0.42}FeCo_3Sb_{12}}$, in comparison with data of almost divalent magnetic $\mathrm{Eu_{0.83}Fe_4Sb_{12}}$. The absorption edge spectra obtained (Fig. 3(a)) are characterised by a double peak structure, evidencing non-integer valence of the Eu ion. Spectral weight is centred around $E_1 = 6973$ eV and $E_2 = 6982$ eV, with no substantial dependence on the particular compound. While the former peak is associated with the 2+ state of Eu, the latter corresponds to Eu^{3+}. The magnetic behaviour therefore varies between a stable magnetic state and a non-magnetic ground state, respectively. Results of a standard analysis of the present data yield an overall valence change from $\nu = 2.25$ ($\mathrm{Eu_{0.83}Fe_4Sb_{12}}$) to $\nu = 2.55$ ($\mathrm{Eu_{0.42}FeCo_3Sb_{12}}$). Significant deviations from the 2+ state are usually accounted for in terms of intermediate valence, however, *(i)* the L_{III} edge spectra do not evolve versus temperature and *(ii)* the Fe/Co substitution on a microscopic scale may be resolved in Fe-rich [$\mathrm{TM_4Sb_{12}}$] units with almost divalent Eu (as in $\mathrm{Eu_{0.83}Fe_4Sb_{12}}$) and in Co-rich [$\mathrm{TM_4Sb_{12}}$] units, where the effect of Eu vacancies may drive the compound towards the non-magnetic state. The double random substitution Fe/Co and Eu/vacancy on the macroscopic scale may thus result in a simple average mix of the two Eu valence states. No temperature dependent changes of spectral weight occur for both electronic configurations in the whole series and moreover, the energy separation ΔE between both absorption maxima is larger than 8 eV, independent on temperature and almost independent on the concentration. These experimental facts obviously indicate that $\mathrm{Eu_yFe_{4-x}Co_xSb_{12}}$ is characterised by some sort of mixed valence behaviour.

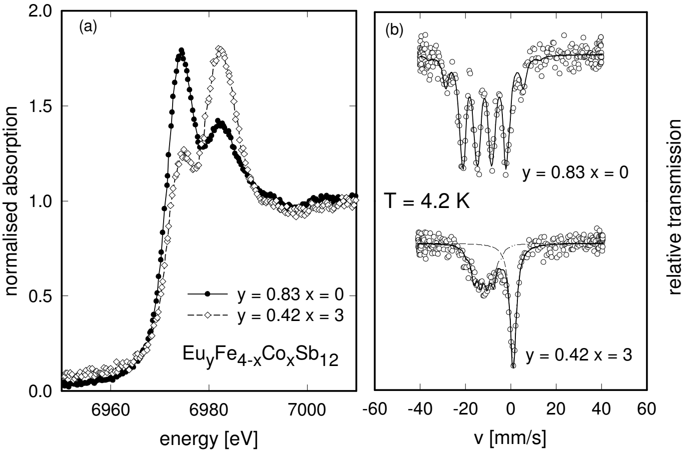

Fig. 3. L_{III} and Mössbauer spectra of $\mathrm{Eu_{0.83}Fe_4Sb_{12}}$ and $\mathrm{Eu_{0.42}FeCo_3Sb_{12}}$.

Mössbauer measurements for $Eu_{0.83}Fe_4Sb_{12}$ (Fig. 3(b)) reveal just a single resonance line in the paramagnetic state [16], indicating an almost divalent nature of the Eu ion. This Eu^{2+} line splits magnetically at 4.2 K due to the ordering of the Eu^{2+} moments at low temperatures ($T_{\mathrm{mag}} = 84$ K). In the case of $Eu_{0.42}FeCo_3Sb_{12}$ one encounters distinct differences: as shown in Fig. 3(b) a second line appears at an isomer shift of 0 mm/s (Eu^{3+}), inferring a mixed valence state with a ratio of $Eu^{2+}/Eu^{3+} = 1$, in fine agreement with the above mentioned L_{III} data ($\nu = 2.55$). This result excludes any dynamic valence fluctuations within this series. As expected, the Eu^{2+} component of the spectrum of $Eu_{0.42}FeCo_3Sb_{12}$ is magnetically split due to the ordering of the Eu^{2+} moments and results in a $B_{\mathrm{eff}} = -11$ T.

3.3. Kondo effect and hopping conductivity in Yb-based skutterudites

Besides the number of charge carriers, magnetic scattering processes modify the temperature dependence of transport coefficients. Simple temperature independent spin-disorder scattering, however, is diversified by crystalline electric field effects and/or by Kondo interaction. The latter yields at somewhat elevated temperatures a negative logarithmic contribution to $\rho(T)$ but can cause at low temperatures a Fermi-liquid behaviour, evidenced by a T^2 behaviour of $\rho(T)$. To illustrate such features, $\rho(T)$ normalised to room temperature is plotted in Fig. 4(a) for a number of filled skutterudites containing Ce and Yb. For a purpose of comparison, $La_{0.8}Fe_4Sb_{12}$ is added. Most obvious, $Yb_{0.22}Ce_{0.3}Fe_3NiSb_{12}$ exhibits a minimum in $\rho(T)$ and at lower temperature a logarithmic increase. Both features are typical signs for Kondo interaction of charge carriers with the independently behaving magnetic moments of Ce and Yb. $\rho(T)$ of $Yb_{0.8}Fe_4Sb_{12}$ is characterised by a pronounced curvature around 100 K followed by a significant decrease of $\rho(T)$ towards lower temperatures and eventually, a T^2 behaviour reflects a Fermi-liquid ground state, whereas for $Ce_{0.8}Fe_4Sb_{12}$ hints of pronounced Kondo interactions are absent at low temperatures. It is interesting to note that even $La_{0.8}Fe_4Sb_{12}$, with non-magnetic La, does not render a simple $\rho(T)$ behaviour, dominated by phonon scattering.

The temperature dependent resistivity of $Yb_yRh_4Sb_{12}$, $y \approx 0.1$ and $Yb_yIr_4Sb_{12}$, $y \approx 0.02$ is shown in Fig. 4(b), again in a normalised representation. Both compounds display a semiconducting-like behaviour where the resistivity increases over some orders of magnitude from room temperature to 4 K. Applying an activation-type model to describe $\rho(T)$ in this case, *i.e.*, $\rho = \rho_0 \exp(\Delta E/2k_{\mathrm{B}}T)$, allows us to estimate the gap width ΔE of the electronic density of states (DOS) at the Fermi energy E_{F}. A least squares fit to the data above about 100 K reveals $\Delta E = 368$ K for TM = Rh and $\Delta E = 277$ K for TM = Ir. A shoulder in $\rho(T)$ around 50 K, however, marks

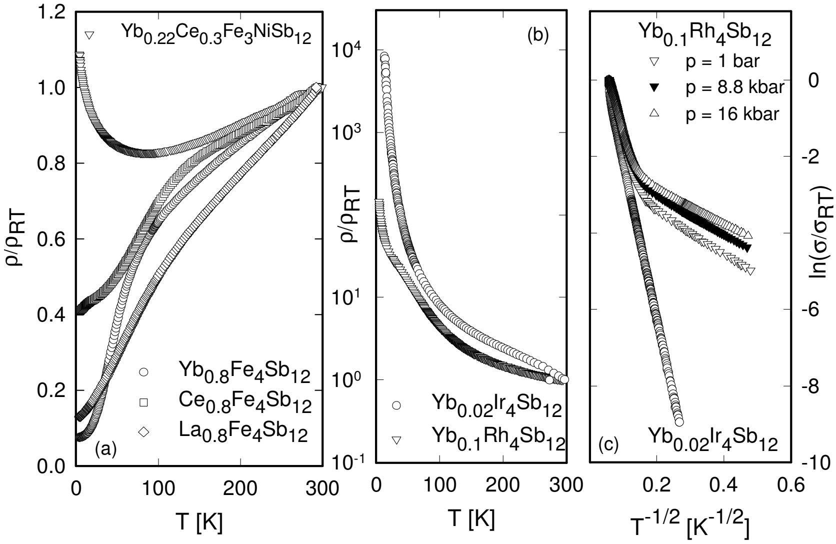

Fig. 4. (a) Normalised resistivity ρ/ρ_{RT} of $RE_yTM_4Sb_{12}$, RE = La, Ce, Yb; TM = Fe, Ni. (b) Normalised resistivity of $Yb_{0.02}Ir_4Sb_{12}$ and $Yb_{0.1}Rh_4Sb_{12}$. (c) Normalised conductivity σ/σ_{RT} vs. $T^{-1/2}$ of $Yb_{0.02}Ir_4Sb_{12}$ and $Yb_{0.1}Rh_4Sb_{12}$ at various values of pressure.

the end of the validity of an activation type behaviour (Fig. 4(b)). In order to account for the temperature range below, we tried to invoke Mott's model of variable range hopping [17], *i.e.*,

$$\sigma = \sigma_0 \exp\left[-\left(\frac{T_0}{T}\right)^n\right], \tag{1}$$

where $\sigma \equiv 1/\rho$, σ_0 is a material constant, T_0 is a characteristic temperature of the system and $n = 1/4$. Least squares fits of Eqn. 1 to the data yield reasonable agreement only in a narrow temperature interval. An exponent $n = 1/2$, on the contrary, describes the conductivity data over a substantial larger temperature range as it is obvious from a plot of $\ln(\sigma/\sigma_{RT})$ vs. $T^{-1/2}$ for both $Yb_{0.1}Rh_4Sb_{12}$ and $Yb_{0.02}Ir_4Sb_{12}$. The characteristic temperatures T_0 are 35 and 1700 K, respectively. The exponent $n = 1/2$ is appropriate for variable range hopping in the presence of a Coulomb gap [18], *i.e.*, when the single-particle density of states close to the chemical potential is depleted due to the Coulomb interaction between electrons. Pressure applied to $Yb_{0.1}Rh_4Sb_{12}$ (Fig. 4(c)) leaves the general features of the hopping-type conductivity unchanged but the characteristic temperature decreases linearly from 35 K at $p = 1$ bar to about 28 K at $p = 16$ kbar.

4. Thermoelectric performance

4.1. Thermopower

The key parameter for thermoelectric materials is the coefficient of the thermoelectric power S, which should exceed, at least, values of 100 μV/K.

According to Mott's formula of diffusion thermopower [19], *i.e.*,

$$S_{\mathrm{d}} = \frac{\pi^2 k_{\mathrm{B}}^2 T}{3|e|} \frac{1}{N(E_{\mathrm{F}})} \frac{dN(E)}{dE}\bigg|_{E=E_{\mathrm{F}}} \tag{2}$$

the energy derivative $dN(E)/dE$ at the Fermi energy determines both, the absolute values as well as the sign of thermopower. Since $S(T)$ depends also on $N(E_{\mathrm{F}})$, a lower value of charge carriers, at least in a one-band model, will cause larger values of the Seebeck coefficient. Thus, systems with $S \gg 100$ μV/K are traditionally found at the border between metals and semiconductors. Highly correlated electron systems, however, have the ability to generate large $S(T)$ values as well. This phenomenon is related to Kondo interaction, where due to a loss of spin degrees of freedom a narrow resonance (width $\Gamma \sim k_{\mathrm{B}}T_{\mathrm{K}}$) emerges in the vicinity of the Fermi energy, giving rise to huge values of $dN(E)/dE|_{E=E_{\mathrm{F}}}$.

In order to trace both sources for enhanced values of the Seebeck coefficient, Fig. 5 shows $S(T)$ of $\mathrm{REFe_4Sb_{12}}$, RE = La, Pr, Nd. As evidenced in the preceding chapter concerning specific heat, $\mathrm{PrFe_4Sb_{12}}$ shows significant electron correlations, observed from large values of C_p/T. These correlations cause substantially larger $S(T)$ values in $\mathrm{PrFe_4Sb_{12}}$ compared to $\mathrm{LaFe_4Sb_{12}}$ and $\mathrm{NdFe_4Sb_{12}}$ (Fig. 5(a)). Driven by substitutions on both the transition metal and the pnictogen site, changes of the carrier concentration can be achieved. The reduction of the carrier concentration due to the Fe/Ni substitution has two different consequences (compare Fig. 5(b)): *(i)* absolute $S(T)$ increases, reaching extraordinarily large room temperature values of 190 μV/K ($\mathrm{Pr_{0.2}Fe_{2.5}Ni_{1.5}Sb_{12}}$) and *(ii)* the sign of thermopower changes from plus to minus, referring to a change of the carrier type from predominantly hole - to electron dominated transport. It is interesting to note that electron correlations are lost upon the Fe/Ni substitution. This follows from the vanishing of the pronounced low temperature structure in $S(T)$.

4.2. Thermal conductivity

In addition to the important contribution of thermopower to the figure of merit, thermal conductivity should be as low as possible. Filled skutterudites provide almost perfect conditions for the requirement above. *(i)* Since skutterudites in general possess just smaller numbers of charge carriers, the electronic contribution λ_{e} to the total thermal conductivity λ is low. *(ii)*

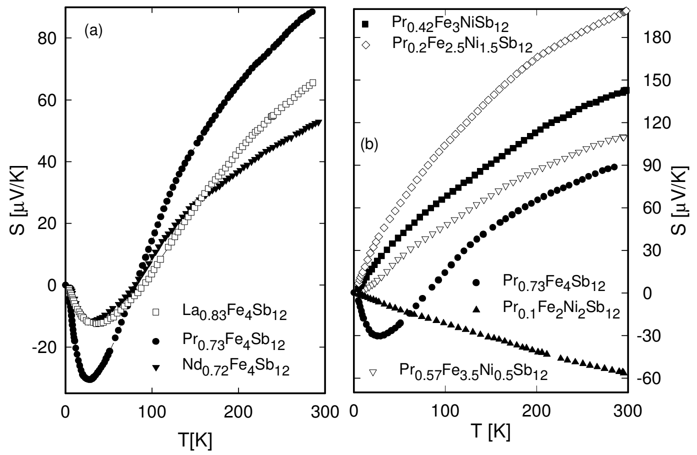

Fig. 5. (a) Temperature dependent Seebeck coefficient $S(T)$ of $\mathrm{RE_yFe_4Sb_{12}}$, RE = La, Pr, Nd. (b) Temperature dependent Seebeck coefficient $S(T)$ of $\mathrm{Pr_yTM_4X_{12}}$, TM = Fe, Ni; X = Sb, Sn.

The strong interaction of the heat carrying phonons with the weakly bound electropositive element dramatically reduces the lattice thermal conductivity λ_{ph}, and the theoretical minimum thermal conductivity, as *e.g.*, found in glass-like materials, is almost reached.

As an example of an evolution of the thermal conductivity in ternary skutterudites, $\lambda(T)$ of $\mathrm{Nd_yFe_4Sb_{12}}$ is shown in Fig. 6 (a). $\lambda(T)$ of this series lowers extraordinarily as the degree y of the filler element starts to increase. Thus, scattering on this filler element can be considered as origin for such a reduction. In order to quantitatively understand the main mechanisms responsible, $\lambda(T)$ has to be separated into its constituents, *i.e.*, $\lambda = \lambda_{\mathrm{e}} + \lambda_{\mathrm{ph}}$, where λ_{e} and λ_{ph} represent the electronic and the lattice thermal conductivity, respectively. Both individual contributions, however, are limited by a number of scattering processes. According to Matthiessen's rule, the thermal resistivity $W_{\mathrm{e(ph)}} \equiv 1/\lambda_{\mathrm{e(ph)}}$ reads

$$1/\lambda_{\mathrm{e}} \equiv W_{\mathrm{e}} = W_{\mathrm{e},0} + W_{\mathrm{e,ph}} + W_{\mathrm{e,mag}} \tag{3}$$

where the subscripts $(e,0)$, (e,ph) and (e,mag) refer to scattering of charge carriers on static imperfections, phonons and magnetic moments, respectively. For simple metals, the electronic thermal conductivity is related to the electrical resistivity via the Wiedemann Franz law: $\lambda_{\mathrm{e}} \approx L_0 T/\rho$ where $L_0 = 2.45 \times 10^{-8}$ $\mathrm{W\Omega/K^2}$. Taking this into account, the total measured quantity can be separated into the electronic and the lattice part. Results of such a procedure are shown in Fig. 6(b) for $\mathrm{Nd_{0.2}Fe_4Sb_{12}}$. This analysis

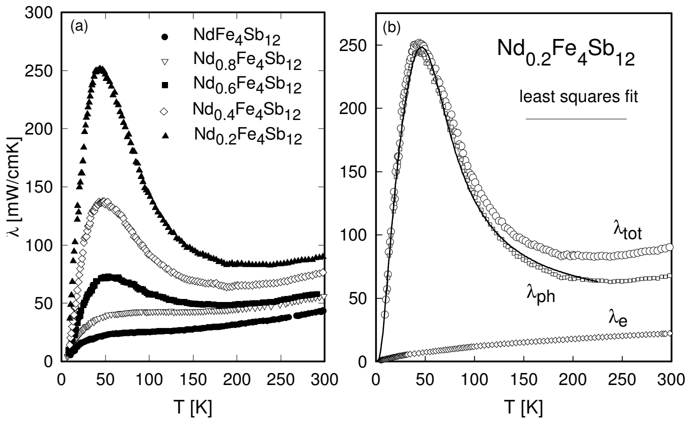

Fig. 6. (a) Temperature dependent thermal conductivity $\lambda(T)$ of $Nd_yFe_4Sb_{12}$. (b) $\lambda(T)$ of $Nd_{0.2}Fe_4Sb_{12}$ (large open symbols). The electron and the phonon contribution λ_e and λ_{ph} are shown with smaller symbols. The solid line is a least squares fit according to Eq. (5) and (6).

indicates that the lattice contribution λ_{ph} is primarily responsible for carrying heat in this material. $\lambda_e(T)$ smoothly increases, but is reduced by a factor of two when proceeding from $Nd_{0.2}Fe_4Sb_{12}$ to $NdFe_4Sb_{12}$. This change is associated with the lower charge carrier concentration of $NdFe_4Sb_{12}$ with respect to $Nd_{0.2}Fe_4Sb_{12}$. While in the former the holes of $[Fe_4Sb_{12}]$ are compensated to a large extent, this does not hold for the latter.

Using Matthiessens rule, λ_{ph} reads:

$$1/\lambda_{\mathrm{ph}} \equiv W_{\mathrm{ph}} = \sum W_{ph,i}\,, \tag{4}$$

where $\sum W_{ph,i}$ represents the most significant scattering processes present in filled skutterudites, giving rise to different temperature dependencies. Within the Debye approximation, λ_{ph} can be expressed as

$$\lambda_{\mathrm{ph}} = CT^3 \int\limits_0^{\theta_{\mathrm{D}}/T} \frac{\tau_c x^4 \exp(x)}{[\exp(x)-1]^2}dx\,, \tag{5}$$

where $x = \hbar\omega/k_{\mathrm{B}}T$, ω is the phonon frequency and θ_{D} is the Debye temperature. τ_c is the total relaxation time given by

$$\tau_c^{-1} = \tau_{\mathrm{B}}^{-1} + \tau_{\mathrm{D}}^{-1} + \tau_{\mathrm{U}}^{-1} + \tau_{\mathrm{e}}^{-1} \tag{6}$$

τ_{B}, τ_{D}, τ_{U}, τ_{e} are the relaxation times for boundary scattering, defect scattering, Umklapp processes and electron scattering, respectively.

Taking into account these most important relaxation processes and their temperature dependencies [20] allows us to describe the experimentally derived lattice thermal conductivity. A least squares fit (solid line, Fig. 6(b)) reveals excellent agreement with the data. The evolution from $Nd_{0.2}Fe_4Sb_{12}$ to $NdFe_4Sb_{12}$ shows that primarily τ_D contributes to the observed dramatic reduction of the thermal conductivity, which nicely agrees with the qualitative picture concerning the rattling mode of the rare earth ions in the oversized cage of the skutterudite structure.

5. Summary

Filled skutterudites can be considered as promising materials for thermoelectric applications, behaving as phonon-glass-electron-crystals. This refers to thermal properties similar to those of glass, and electrical transport similar to that in crystalline materials. Very recently, *figure of merit* values above one were reported for skutterudites based on Eu ($ZT \approx 1.1$ at $T = 700$ K) [21] or on Yb ($ZT \approx 1.2$ at $T = 700$ K) [22]. Many of such materials exhibit strong electron correlations, which may further push the *figure of merit* to even larger values.

Research supported by the Austrian FWF-P12899 and P13778 as well as by NEDO (Japan) as an international joint research project.

REFERENCES

[1] G.S. Nolas, *et al.*, *Annu. Rev. Mater. Sci.* **29**, 89 (1999) and references therein.

[2] see *e.g.*: Y. Aoki, *et al.*, *Phys. Rev. B* **65**, 064446/1 (2002) and refs therein.

[3] G.A. Slack, V. Tsoukala, *J. Appl. Phys.* **76**, 1665 (1994).

[4] W. Jeitschko, D.J. Braun, *Acta Crystallogr.* **B33**, 3401 (1977).

[5] V. Keppens, *et al.*, *Nature* **395**, 876 (1998).

[6] I. Shirotani, *et al.*, *Phys. Rev.* **B56**, 7866 (1997).

[7] N. Takeda, M. Ishikawa, *J. Phys. Soc. Jpn.* **69**, 868 (2000).

[8] C. Sekine, *et al.*, *Phys. Rev. Lett.* **79**, 3218 (1997).

[9] E.D. Bauer, *et al.*, *Phys. Rev.* **B** (2002) in press.

[10] Y. Nakanishi, *et al.*, *Phys. Rev.* **B63**, 184429 (2001).

[11] H. Sato, *et al.*, *Physica B* **281–281**, 306 (2000).

[12] T.D. Matsuda, *et al.*, *Physica B* **281–282**, 220 (2000).

[13] H. Sugawara, *et al.*, *J. Magn. Magn. Mater.* **226–230**, 48 (2001).

[14] E. Bauer *et al.*, to be published.

[15] K.D. Schotte, U. Schotte, *Phys. Lett.* **55A**, 38 (1975).

[16] E. Bauer *et al.*, *Phys. Rev.* **B63**, 224414-1 (2001).

[17] N.F. Mott, *J. Non-Cryst. Solids*, **1**, (1968) 1.

[18] A.L. Efros, B.I. Shklovskii, *J. Phys.* **C8**, L49 (1975).

[19] J.S. Dugdale, *The Electrical Properties of Metals and Alloys*, Edward Arnold, London 1977.

[20] J. Callaway, *Phys. Rev.* **122**, 787 (1961).

[21] G.A. Lamberton *et al.*, *Appl. Phys. Lett.* **80**, 598 (2002).

[22] G.S. Nolas *et al.*, *Appl. Phys. Lett.* **77**, 1 (2000).